Widefield subsurface microscopy of integrated circuits

Fatih Hakan Köklü[1*], Justin I. Quesnel[1], Anthony N. Vamivakas[1,2], Stephen B. Ippolito[1,3], Bennett B. Goldberg[1], and M. Selim Ünlü[1]

[1]*Department of Physics and Electrical and Computer Engineering and the Photonics Center, Boston University, 8 Saint Mary's Street, Boston, Massachusetts 02215*
[2]*Cavendish Laboratory, University of Cambridge, JJ Thompson Avenue, Cambridge, UK*
[3]*IBM T. J. Watson Research Center, Yorktown Heights, New York 10598*

hakan@bu.edu

Abstract: We apply the numerical aperture increasing lens technique to widefield subsurface imaging of silicon integrated circuits. We demonstrate lateral and longitudinal resolutions well beyond the limits of conventional backside imaging. With a simple infrared widefield microscope ($\lambda_0 = 1.2\mu$m), we demonstrate a lateral spatial resolution of 0.26μm ($0.22\lambda_0$) and a longitudinal resolution of 1.24μm ($1.03\lambda_0$) for backside imaging through the silicon substrate of an integrated circuit. We present a spatial resolution comparison between widefield and confocal microscopy, which are essential in integrated circuit analysis for emission and excitation microscopy, respectively.

OCIS codes: (110.0180) Microscopy; (120.4630) Optical inspection; (180.1790) Confocal microscopy

References and links

1. C. Xu and W. Denk, "Two-photon optical beam induced current imaging through the backside of integrated circuits," Appl. Phys. Lett. **71,** 2578–2580 (1997).
2. E. Ramsay, D. T. Reid, and K. Wilsher, "Three-dimensional imaging of a silicon flip chip using the two-photon optical-beam induced current effect," Appl. Phys. Lett. **81,** 7–9 (2002).
3. International Technology Roadmap for Semiconductors Update, 2006.
4. S. B. Ippolito, B. B. Goldberg, and M. S. Ünlü, "High spatial resolution subsurface microscopy," Appl. Phys. Lett. **78,** 4071–4073 (2001).
5. S. M. Mansfield and G. S. Kino, "Solid immersion microscope," Appl. Phys. Lett. **57,** 2615–2617 (1990).
6. S. B. Ippolito, S. A. Thorne, M. G. Eraslan, B. B. Goldberg, M. S. Ünlü, and Y. Leblebici, "High spatial resolution subsurface thermal emission microscopy," Appl. Phys. Lett. **84,** 4529–4531 (2004).
7. E. Ramsay, N. Pleynet, D. Xiao, R. J. Warburton, and D. T. Reid, "Two-photon optical-beam-induced current solid-immersion imaging if a silicon flip chip with a resolution of 325 nm," Opt. Lett. **30,** 26–28 (2005).
8. E. Ramsay, K. A. Serrels, M. J. Thomson, A. J. Waddie, M. R. Taghizadeh, R. J. Warburton, and D. T. Reid, "Three-dimensional nanoscale subsurface optical imaging of silicon circuits," Appl. Phys. Lett. **90,** 131101 (2007).
9. Z. Liu, B. B. Goldberg, S. B. Ippolito, A. N. Vamivakas, M. S. Ünlü, and R. Mirin, "High resolution, high collection efficiency in numerical aperture increasing lens microscopy of individual quantum dots," Appl. Phys. Lett. **87,** 071905 (2005).
10. A. N. Vamivakas, M. Atatüre, S. T. Dreiser, J. Yilmaz, A. Badolato, A. K. Swan, B. B. Goldberg, A. Imamoglu, and M. S. Ünlü, "Strong extinction of a far-field laser beam by a single quantum dot," Nano Lett. **7,** 2892–2894 (2007).
11. J. B. Pawley, *Hanbook of Biological Confocal Microscopy* 3rd ed., (Springer Press, 2006), p. 209.
12. S. B. Ippolito, B. B. Goldberg, and M. S. Ünlü, "Theoretical analysis of numerical aperture increasing lens microscopy," J. Appl. Phys. **97,** 053105 (2005).

#95145 - $15.00 USD Received 17 Apr 2008; revised 6 Jun 2008; accepted 9 Jun 2008; published 12 Jun 2008

13. M. A. Green and M. Keevers, "Optical properties of intrinsic silicon at 300k," Prog. in Photovol. **3,** 189–192 (1995).
14. T. Wilson and C. Sheppard, *Theory and Practice of Scanning Optical Microscopy* (Academic Press, 1984) p. 28.
15. S. B. Ippolito, P. Song, D. L. Miles, and J. D. Sylvestri, "Angular spectrum tailoring in solid immersion microscopy for circuit analysis," Appl. Phys. Lett. **92,** 101109 (2008).

1. Introduction

Development and implementation of various optical methods for functional defect detection and imaging of silicon integrated circuits (IC) have been crucial for analysis and advancement of microelectronics [1, 2]. Optical analysis is accomplished by either excitation of circuit elements or collection of emission and scattering from the circuit. A correlated reflection image is necessary for registration of the analytical information to the circuit layout. Current IC technology includes a multitude of opaque metal layers thus hindering frontside optical imaging of buried device layers. Therefore, nearly all optical analysis and inspection (reflection microscopy) techniques require backside imaging. In backside imaging, optical absorption in silicon substrate limits the utilized optical spectrum to $\lambda_0 \geq 1\mu$m which results in limited lateral resolution in conventional microscopy - commercial systems typically provide $\sim 1\mu$m. However, Si IC fabrication technology, currently at the 65nm process node and scaling down, requires imaging resolution well beyond the capability of state-of-the-art conventional backside microscopy through the planar substrate surface [3]. We have recently developed Numerical Aperture Increasing Lens (NAIL) microscopy [4] that allows for high resolution backside imaging of silicon ICs. A silicon NAIL placed on the backside of a Si substrate effectively transforms the NAIL and the planar sample into an integrated solid immersion lens [5] increasing the numerical aperture (NA) by a factor of the square of the refractive index *n*, to a maximum NA of 3.5 in silicon. An immediate impact of this immersion technique has been observed in high-resolution metrology and failure analysis in the semiconductor industry [6, 7, 8] as well as fundamental studies in semiconductor nanostructures and quantum dots [9, 10].

Backside imaging through the planar substrate surface is very poor for longitudinal imaging since the confocal depth, $\Delta z = \frac{\lambda_0}{n(1-cos\theta)}$, approximately scales inversely with the square of NA [11]. This results in $\Delta z \sim 28\mu$m for NA = 0.5 and $\lambda_0 = 1\mu$m. This limitation is very important when imaging layered samples such as silicon ICs in which structures in out-of-focus layers blurs the image and reduces visibility. The lack of depth resolution at the length scale of IC layers represents a significant restriction even in confocal scanning and renders widefield imaging nearly impossible. Thus, improvements in both lateral and longitudinal resolution can have significant impact on optical analysis and inspection techniques.

In this paper, we demonstrate very high lateral and longitudinal resolution using a simple infrared widefield microscope and a NAIL in backside silicon IC imaging. We find a lateral resolution of 0.26μm ($0.22\lambda_0$) and a longitudinal resolution of 1.24μm ($1.03\lambda_0$) while imaging subsurface features of an IC from the backside at $\lambda_0 = 1.2\mu$m.

2. Experiment

We constructed a custom microscope capable of widefield and confocal imaging for comparison of different NAIL microscopy modalities as shown in Fig. 1. The confocal setup is a single-path, reflection-mode fiber-optical scanning microscope utilizing a single mode fiber coupled laser diode ($\lambda_0 = 1.3\mu$m) and a 2x2 optical coupler instead of a beamsplitter. For coupling in and out of the single mode fiber, we use a collimating objective with matching NA to the single mode fiber and a second objective with NA = 0.26 is used for illumination and collection. A piezo stage is used to form an image by scanning the sample with the NAIL.

#95145 - $15.00 USD Received 17 Apr 2008; revised 6 Jun 2008; accepted 9 Jun 2008; published 12 Jun 2008

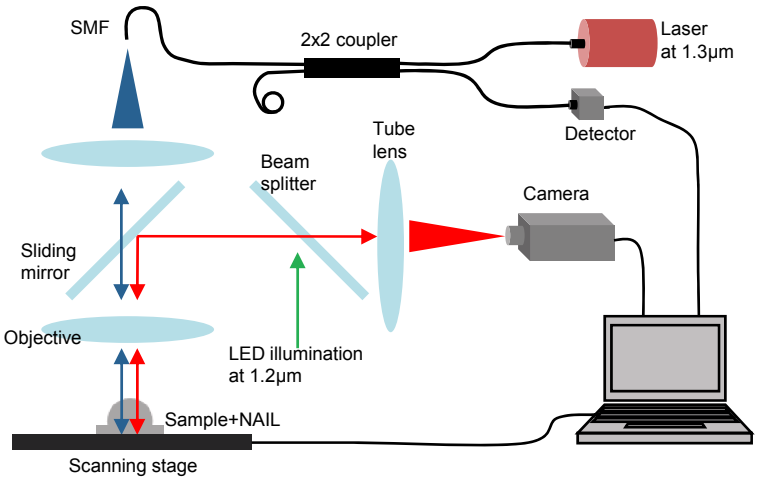

Fig. 1. (Color online) Experimental setup. A sliding mirror provides switching between confocal and widefield microscopes. When the sliding mirror is out, in confocal imaging, illumination and detection is done through the same fiber using a 2x2 optical coupler. When the sliding mirror is in, the sample is illuminated with an LED array and the image is captured using an InGaAs camera.

The widefield microscope body consists of a zoom module, a tube lens, and utilizes the same objective as in confocal for NAIL imaging (NA = 0.26) and a 0.4 NA objective for conventional backside microscopy without a NAIL. The illumination source is an LED array with a peak wavelength of 1.2μm. The collected radiation is imaged onto an InGaAs camera (320x240 pixels).

The NAIL used in this work is an undoped silicon hemisphere with radius R = 1.61mm. The substrate thickness (X) for aplanatic imaging with a hemispherical NAIL is $X = R/n$ where n is the refractive index at operating wavelength [12]. Thus $X = 457\mu$m ($X = 460\mu$m) for $\lambda_0 = 1.2\mu$m ($\lambda_0 = 1.3\mu$m), the center wavelength of widefield (confocal) imaging [13].

The sample is a custom IC with 4 metal and 2 polysilicon layers fabricated at Austriamicrosystems by a 0.35μm process. The substrate thickness was reduced to 458$\pm$2μm for aplanatic imaging at operating wavelengths by chemical mechanical polishing that provides a flat and smooth surface, crucial for NAIL microscopy. Some samples were polished to 492$\pm$2μm to test the performance degradation of NAIL imaging away from optimal substrate thickness.

Imaging is performed on passive calibration structures designed to have different linewidths and spacings, and embedded into the first polysilicon layer of the IC. The six passive test structures have δ values of 0.35, 0.6, 0.9, 1.2, 1.5 and 2μm to quantify the resolution performance of our confocal and widefield imaging systems (See Fig. 2(a)). We included horizontal and vertical lines in the upper metal layers to test the three dimensional imaging capabilities. Figures 2(b) and 2(c) display frontside and backside conventional images of the area of the sample with all six test structures, and Figs. 2(d) and 2(e) display the magnified images of those with $\delta = 0.9\mu$m and 0.35μm. Figure 2(f) shows the backside images of the corresponding test structures using a NAIL and a sample with optimum substrate thickness.

3. Results

The objectives used for images in Figs. 2(b,d), 2(c,e) and 2(f) have NA = 0.9, 0.4 and 0.26, respectively. As seen in the upper magnified images in Figs. 1(d) and 1(e), 0.9μm lines that

#95145 - $15.00 USD Received 17 Apr 2008; revised 6 Jun 2008; accepted 9 Jun 2008; published 12 Jun 2008

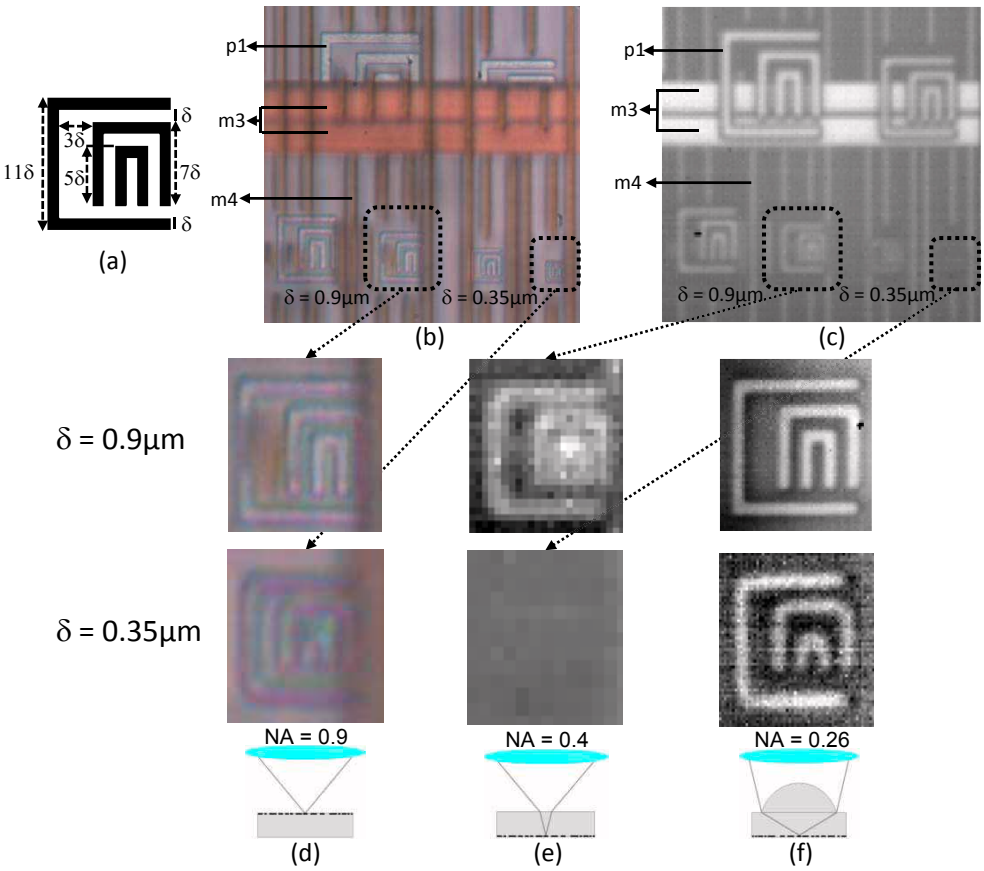

Fig. 2. (Color online) (a) Drawing of the test structure. The sample has 6 test structures scaled with δ = 0.35, 0.6, 0.9, 1.2, 1.5 and 2μm. (b) Front side image of the sample with a commercial visible wavelength optical microscope. (c) Backside image of the sample with the NIR ($\lambda_0 = 1.2\mu$m) widefield microscope without a NAIL. (d) The magnified frontside images of the test structures with δ = 0.9μm (upper) and δ = 0.35μm (lower) taken with the visible microscope. (e) The magnified backside images of the test structures with δ = 0.9μm (upper) and δ = 0.35μm (lower) taken with the NIR microscope without a NAIL. (f) Backside image of the test structures with δ = 0.9 and 0.35 μm, respectively, using the NIR widefield microscope and a NAIL with an optimum substrate thickness of 458μm. Notice the upper layers in (b) and (c).

are visible in frontside imaging are not resolved by conventional backside microscopy. However, NAIL provides a clear image of this structure in Fig. 2(f). The images of the test structure with δ = 0.35μm emphasize the advantage of backside imaging with a NAIL. The test structure ($\delta = 0.35\mu$m) clearly seen by NAIL microscope (at $\lambda_0 = 1.2\mu$m, Fig. 2(f)) is completely indistinguishable by conventional backside imaging (Fig. 2(e) lower) and even beyond the resolution limit of frontside microscope despite the significantly shorter visible wavelength used (Fig. 2(d) lower).

To quantify the performance of imaging with each microscope, a line scan is taken at the top edge of the test structure with $\delta = 2\mu$m. An error function is fit to the data for each case and line spread functions (LSF) shown in Fig. 3 are extracted. With the optimum substrate thickness, we achieve 0.26μm (0.22λ_0) and 0.20μm (0.15λ_0) resolutions with widefield and confo-

#95145 - $15.00 USD Received 17 Apr 2008; revised 6 Jun 2008; accepted 9 Jun 2008; published 12 Jun 2008

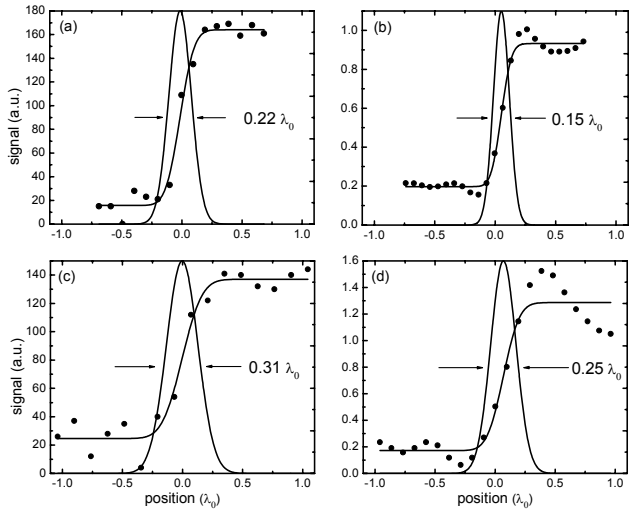

Fig. 3. (a) Data and fit to error function with the line spread function is shown using the widefield microscope for an optimum substrate thickness of 458μm. (b) Same as (a) but with a confocal microscope. (c) Same as (a) but with a non-optimum substrate thickness of 492μm. (d) Same as (c) but with a confocal microscope. All x-axes are normalized to the corresponding wavelengths; $\lambda 0 = 1.2\mu$m for widefield and $\lambda 0 = 1.3\mu$m for confocal microscopy.

cal microscopes, respectively, according to the Houston criterion. For non-optimum substrate thickness ($\sim 35\mu$m larger than optimum), the resolutions for confocal and widefield imaging degrades to 0.37μm (0.31λ_0) and 0.32μm (0.25λ_0), respectively. The data for the confocal case for both substrate thicknesses exhibit fringes due to coherent imaging [14]. Although this effect degrades the quality of the fits, to make a fair comparison between confocal and widefield imaging, both curves should be fit to the same function.

In conventional widefield microscopy, there is no out-of-focus light rejection, and thus no ability to image separate layers. As seen in Fig. 2(c), all metal and poly layers are simultaneously visible. However, NAIL microscopy can overcome this, since it provides a more pronounced improvement in longitudinal than lateral imaging due to the inverse square dependence of confocal depth on NA. NAIL microscopy allows for very tight focusing and light from other layers blurs rapidly providing a nearly uniform background [15]. By subtracting this background, we achieve distinguishable images of features in individual layers with relatively high contrast. As seen in the image of the test structure with δ = 1.5μm in Fig. 4(a), a thick wire of metal3 passing above it makes imaging from frontside impossible. On the other hand, we can selectively focus on different layers of the IC when imaging from backside with a NAIL. The microscope is focused on poly1, metal3 and metal4 layers respectively in Figs. 4(b), 4(c) and 4(d). The separation between poly1 and metal3 layers is typically 2.65μm according to the manufacturer. As displayed in Fig. 4(b), the test structure in poly1 layer is imaged individually. In addition, as seen in Figs. 4(c) and 4(d), poly1 layer is virtually invisible when imaging metal3 and metal4 layers. However, these two layers having a typical separation of 1μm cannot be imaged separately.

Figure 5 shows linecuts taken through the top line of the test structure with δ = 1.5μm where there is no other structure above. The linecut taken with the confocal microscope has a FWHM of 0.58μm (0.45λ_0) and that of widefield microscope has a FWHM of 1.24μm (1.03λ_0). It

#95145 - $15.00 USD Received 17 Apr 2008; revised 6 Jun 2008; accepted 9 Jun 2008; published 12 Jun 2008

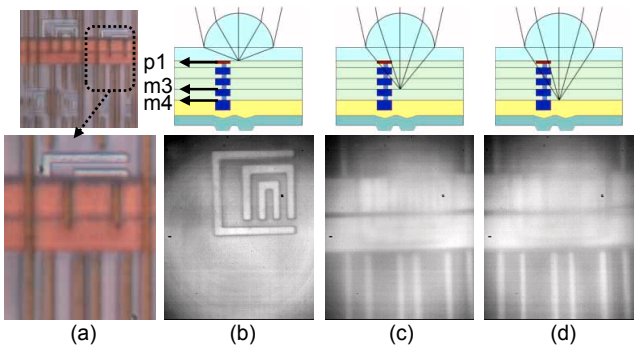

Fig. 4. (Color online) (a) Frontside image of the test structure with δ = 1.5μm taken with the visible wavelength microscope shows all the layers together. (b) Isolated image of the same test structure is easily seen when focused at the poly1 layer. (c) The same area now focused at the metal3 layer. (d) The same area when focused at the metal4 layer. In (b) metal3 and metal4 layers are not seen and in (c) and (d) poly1 layer disappears. However, metal3 and metal4 layers cannot be imaged separately. According to the manufacturer, typical separation between poly1 and metal3 is 2.65μm whereas the separation between metal3 and metal4 is 1μm. In the illustrations, layer and interlayer thicknesses are in scale, but substrate and NAIL thickness and the refraction angles are not.

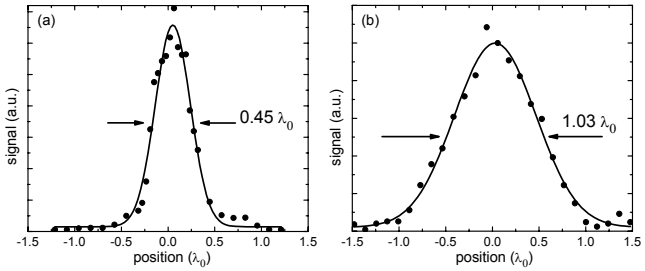

Fig. 5. Longitudinal linecut taken (a) with the confocal microscope and (b) with the wide-field microscope.

should be emphasized that the signal used for widefield imaging is generated with background subtraction.

4. Conclusion

In conclusion, we have made significant improvements in widefield and confocal microscopy using the NAIL technique. We have demonstrated record lateral resolutions of 0.26μm (0.22λ_0) and 0.20μm (0.15λ_0) while imaging multi-layered silicon ICs using widefield and confocal microscopy, respectively. In addition, we demonstrate vertical sectioning of stacked structures with a longitudinal resolution of 1.24μm (1.03λ_0) using a simple widefield microscope. These results exhibit that using a NAIL in the widefield configuration provides a simple, yet effective solution for silicon IC inspection.

The authors wish to thank Prof. Thomas Bifano, Dr. Jinhong Kim and Dr. David Bergstein for their help at sample preparation. This work was supported by Air Force Office of Scientific Research under grant MURI F-49620-03-1-0379.

#95145 - $15.00 USD Received 17 Apr 2008; revised 6 Jun 2008; accepted 9 Jun 2008; published 12 Jun 2008